Development 138, 2987-2998 (2011) doi:10.1242/dev.066589


# A role for Notch signaling in trophoblast endovascular invasion and in the pathogenesis of pre-eclampsia

**Nathan M. Hunkapiller[1,2], Malgorzata Gasperowicz[3], Mirhan Kapidzic[1,2], Vicki Plaks[4], Emin Maltepe[1,5,6,7], Jan Kitajewski[8,9,10], Jay C. Cross[3] and Susan J. Fisher[1,2,4,5,11,12,*]**

## SUMMARY

Placental trophoblasts (TBs) invade and remodel uterine vessels with an arterial bias. This process, which involves vascular mimicry, re-routes maternal blood to the placenta, but fails in pre-eclampsia. We investigated Notch family members in both contexts, as they play important roles in arterial differentiation/function. Immunoanalyses of tissue sections showed step-wise modulation of Notch receptors/ligands during human TB invasion. Inhibition of Notch signaling reduced invasion of cultured human TBs and expression of the arterial marker *EFNB2*. In mouse placentas, Notch activity was highest in endovascular TBs. Conditional deletion of *Notch2*, the only receptor upregulated during mouse TB invasion, reduced arterial invasion, the size of maternal blood canals by 30-40% and placental perfusion by 23%. By E11.5, there was litter-wide lethality in proportion to the number of mutant offspring. In pre-eclampsia, expression of the Notch ligand JAG1 was absent in perivascular and endovascular TBs. We conclude that Notch signaling is crucial for TB vascular invasion.

**KEY WORDS: Endovascular Invasion, Notch, Pre-eclampsia, Trophoblast**

## INTRODUCTION

Human placentation involves unique interactions between embryonic/fetal cytotrophoblasts (CTBs) and maternal cells. CTBs that arise from the placental surface colonize the uterine wall and resident maternal vessels (Fig. 1A), a process that requires aggressive invasion of maternal tissues (Fisher et al., 1989; Librach et al., 1991). During interstitial invasion, CTBs commingle with decidual, myometrial and immune cells. During endovascular invasion, CTBs breach maternal spiral arterioles that supply blood to the placenta. Subsequently, they replace the maternal endothelium and regions of the smooth muscle wall, creating a novel chimeric vasculature composed of maternal and fetal cells, a process that greatly increases arteriole diameter. By contrast, CTBs form only superficial connections with uterine veins. These remarkable cell-cell interactions are accompanied by changes in fundamental aspects of the phenotype of the cells with the net effect of mimicking many aspects of endothelial cells (ECs). They switch on the expression of vascular-type adhesion molecules (Damsky et al., 1992; Zhou et al., 1997), vasculogenic/angiogenic factors (Zhou et al., 2003; Zhou et al., 2002) and Ephrin family members that play a role in arterial function and identity (Red-Horse et al., 2005). The significance of CTB endovascular invasion is illustrated by the fact that this process largely fails in pre-eclampsia (PE).

PE is a serious complication that affects ~7% of first-time pregnancies (Levine et al., 1997; Redman and Sargent, 2005). The mother shows signs of widespread alterations in EC function such as hypertension, proteinuria and edema (Roberts and Lain, 2002). Sometimes fetal growth is impaired. In PE, the extent of CTB interstitial invasion is variable, but frequently shallow; endovascular invasion is consistently rudimentary (Brosens et al., 1972; Naicker et al., 2003; Zhou et al., 2007), resulting in increased vascular resistance and decreased placental perfusion (Matijevic and Johnston, 1999). The PE syndrome reveals the significance of CTB differentiation/invasion. Biopsies of the uterine wall of individuals with PE show that invasive CTBs fail to upregulate receptors that promote invasion and/or assumption of an EC-like phenotype (Zhou et al., 2003; Zhou et al., 2002). The upstream regulatory mechanisms that are responsible for these defects remain enigmatic. Thus, ligands/receptors that are involved in vascular patterning are of interest.

The Notch signaling pathway governs differentiation and function during cell-cell contact in many tissues (Bianchi et al., 2006; Miele, 2006) with particularly important roles in vascular patterning (Roca and Adams, 2007; Swift and Weinstein, 2009). Mechanistically, Notch receptors operate both on the cell surface to receive activating signals and within the nucleus as transcriptional modulators (Alva and Iruela-Arispe, 2004; Kopan and Ilagan, 2009). The core mammalian pathway is a conserved family of four transmembrane receptors (NOTCH1-4) and five ligands (DLL1/3/4 and JAG1/2). Binding of receptors and ligands on adjacent cells triggers serial proteolytic cleavages of the receptor, releasing the Notch intracellular domain (NICD) via γ-secretase-mediated processing (Schroeter et al., 1998). Subsequently, cleaved NICD translocates to the nucleus, binds to CBF1/Su(H)/Lag2 family transcription factors, and induces downstream targets such as *Hes* and *Hey* (Weinmaster, 1998).

[1]Center for Reproductive Sciences, University of California, San Francisco, CA 94143, USA. [2]Department of Obstetrics, Gynecology, and Reproductive Sciences, University of California, San Francisco, CA 94143, USA. [3]Department of Comparative Biology and Experimental Medicine, Faculty of Veterinary Medicine, University of Calgary, Calgary, AB T2N 4N1, Canada. [4]Department of Anatomy, University of California, San Francisco, CA 94143, USA. [5]The Eli and Edythe Broad Center for Regeneration Medicine and Stem Cell Research, University of California, San Francisco, CA 94143, USA. [6]Biomedical Sciences Program, University of California, San Francisco, CA 94143, USA. [7]Department of Pediatrics, University of California, San Francisco, CA 94143, USA. [8]Department of Obstetrics and Gynecology, Columbia University, New York, NY 10032, USA. [9]Department of Pathology, Columbia University, New York, NY 10032, USA. [10]Herbert Irving Comprehensive Cancer Center, Columbia University, New York, NY 10032, USA. [11]Human Embryonic Stem Cell Program, University of California, San Francisco, CA 94143, USA. [12]Sandler-Moore Mass Spectrometry Core Facility, University of California, San Francisco, CA 94143, USA.

*Author for correspondence (sfisher@cgl.ucsf.edu)

**Accepted 11 May 2011**

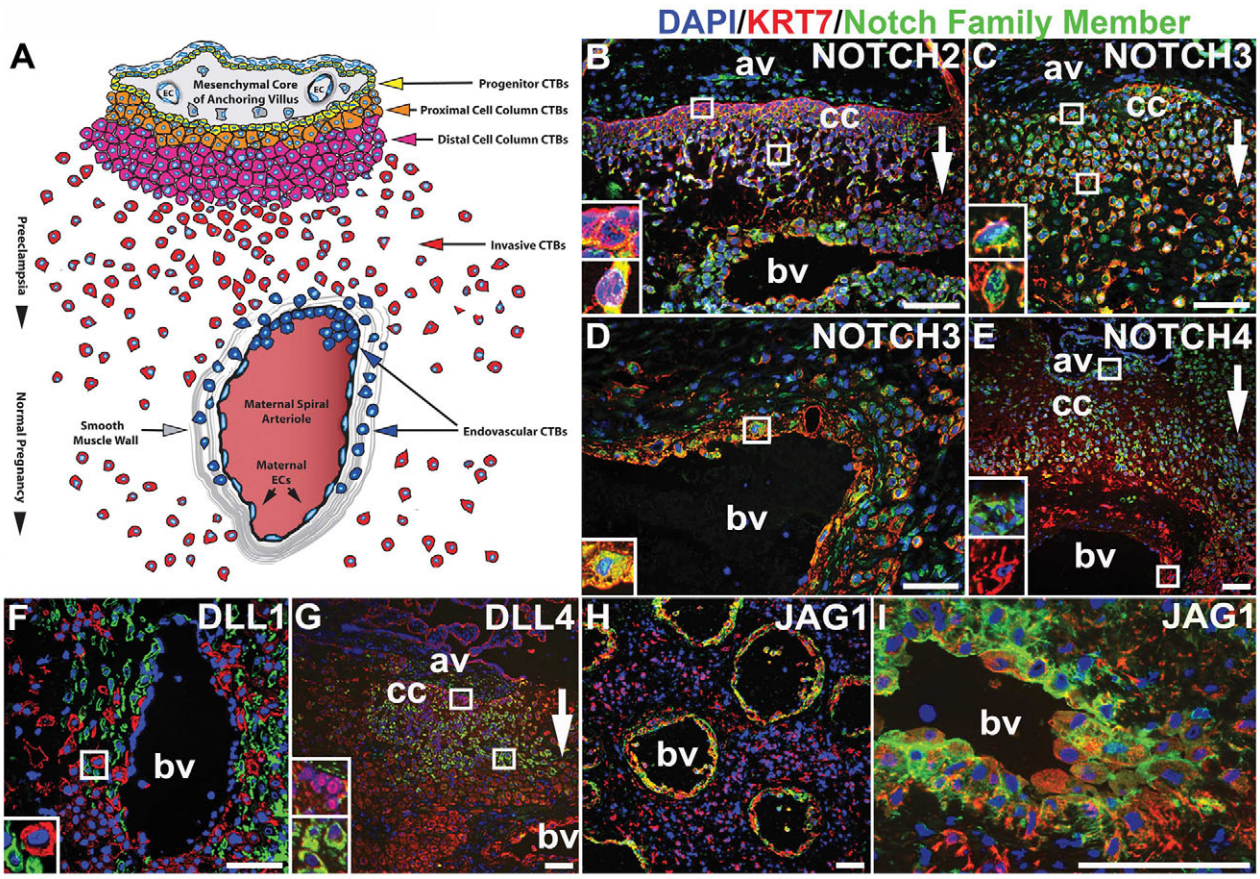


**Fig. 1. CTBs modulated expression of Notch receptors/ligands as they invaded the uterine wall and vasculature.** (**A**) CTBs of anchoring villi (av) differentiate as they invade the maternal uterus. Undifferentiated CTB progenitors (yellow) surround the mesenchymal cores of anchoring villi. These progenitors differentiate as they move into the proximal and distal regions of the cell columns (cc; orange and purple). Invasive CTBs (red) migrate through the uterus. Endovascular CTBs (blue) disrupt the smooth muscle layer of maternal blood vessels (bv), where they also replace ECs. The depth of CTB invasion in normal pregnancy and in pre-eclampsia is indicated by arrowheads. (B-I) Double indirect immunofluorescence was performed on tissue sections of 2nd trimester basal plate biopsies using antibodies that specifically reacted with KRT7 (red), which is expressed exclusively by trophoblasts, and with Notch family members (green). Nuclei were labeled with DAPI (blue). (**B**) CTB progenitors (upper inset) upregulated NOTCH2 expression (lower inset) as they invaded the uterine wall and blood vessels. (**C**,**D**) CTBs expressed NOTCH3 at all stages of differentiation/invasion (insets). (**E**) CTB progenitors and cell columns (upper inset) expressed NOTCH4, which was downregulated in proximity to maternal blood vessels (lower inset). (**F**) DLL1 was expressed by maternal cells in the uterus that associated with CTBs (inset). (**G**) DLL4 immunoreactivity, which was absent in progenitors (upper inset), increased as CTBs entered the cell columns (lower inset) and declined with deeper invasion. (**H**,**I**) CTBs expressed JAG1 only in proximity to maternal spiral arterioles. Scale bars: 100 μm. The direction of invasion is indicated by arrows.

Notch signaling regulates the differentiation of primitive undefined ECs into hierarchical networks by specifying arterial identity. By embryonic days (E) 9.5-11.5 of mouse development, when the primary vascular plexus begins to remodel into arterial and venous networks, *Notch1*/*Notch3*/*Notch4*, *Jag1* and *Dll4* mRNAs are expressed within the developing vasculature. However, by E13.5, their expression is largely confined to arterial endothelium (Villa et al., 2001). Concurrently, *Efnb2* and *Ephb4* emerge as markers of arterial and venous identity, respectively (Wang et al., 1998). In zebrafish, loss of Notch signaling reduced EC *efnb2* expression while simultaneously enhancing *ephb4* expression – evidence that Notch functions upstream of both molecules in specifying vessel identity (Lawson et al., 2001; Zhong et al., 2001). Targeted deletions of Notch family genes produce a variety of vascular defects. Most result in embryonic lethality between E9.5 and E12.5 owing to failed incorporation of the arterial vasculature into the circulation (Roca and Adams, 2007; Swift and Weinstein, 2009). In this context, it is plausible that Notch family members play a role in programming CTB arterial invasion.

In culture, undifferentiated mouse trophoblast stem (TS) cells express all members of the Notch family (Cormier et al., 2004). In vivo, differentiated trophoblasts at the junctional zone (the maternal-fetal interface) express only *Notch2*, which is restricted to a narrow temporal window at midgestation (Nakayama et al., 1997), suggesting that trophoblast differentiation in vivo probably involves significant modulation of Notch expression. As to function, *Notch2*, *Hes2* and *Hes3* are co-expressed in trophoblast giant cells (TGCs), which, along with glycogen trophoblast cells (GlyTCs), carry out interstitial and endovascular invasion. Tetraploid rescue experiments in *Notch2*-deficient mice revealed that placental defects involving the labyrinthian circulatory system are associated with the lethality in *Notch2*-deficient animals (Hamada et al., 2007). However, the mechanisms involved remained elusive. We theorized that defects in trophoblast endovascular invasion contributed to the observed phenotype. Here, we used a combination of mouse and human models to test this theory and to identify PE-associated aberrations in CTB expression of Notch family members.

## MATERIALS AND METHODS

### Human tissue collection

This study was approved by the UCSF Institutional Review Board. Written informed consent was obtained from donors. Biopsies of normal placentas were either fresh-frozen for immunolocalization, paraformaldehyde fixed for in situ hybridization or immediately processed for CTB isolation. Equivalent specimens were obtained from women who experienced either pre-term labor, severe pre-eclampsia, or hemolysis, elevated liver enzymes and low platelets syndrome using clinical criteria and methods we have published (Zhou et al., 2007).

### Immunofluorescence

Fresh-frozen basal plate biopsies were embedded and sectioned as described previously (Zhou et al., 2007). Following fixation in cold methanol:acetone (1:6) for 5 minutes, sections were washed in PBS. Non-specific reactivity was blocked by incubation in 0.3% bovine serum albumin/PBS. They were incubated (overnight at 4°C) with anti-KRT7 (diluted 1:50; produced by the Fisher group), which reacts with all trophoblast populations, and an anti-Notch family member diluted 1:200 [NOTCH1 (Santa Cruz Biotechnology, sc-9011), NOTCH2 (R&D Systems, AF3735), NOTCH3 (Santa Cruz Biotechnology, sc-5593), NOTCH4 (Santa Cruz Biotechnology, sc-8643), JAG1 (Santa Cruz Biotechnology, sc-8303), JAG2 (Santa Cruz Biotechnology, sc-5604), DLL1 (Santa Cruz Biotechnology, sc-9102) and DLL4 (Santa Cruz Biotechnology, sc-18640)]. Subsequently, the sections were rinsed in PBS, incubated with the appropriate species-specific secondary antibody conjugated to either fluorescein (Notch family members) or rhodamine (KRT7), washed in PBS and mounted under Vectashield containing DAPI. Controls were incubated with the primary or secondary antibody alone. Sections were photographed using a Leica DM5000B microscope. Immunostaining with the Tromo-1 antibody (anti-mouse cytokeratin; Developmental Studies Hybridoma Bank) was performed as described above on tissue sections of E12.5 *Notch2*$^{floxl+}$;*Tpbpa-Cre* and *Notch2*$^{floxlflox}$;*Tpbpa-Cre* placentas.

### Immunoblotting

Immunoblotting was performed as previously described (Zhou et al., 2002). Primary antibodies that reacted with NOTCH2 (Developmental Studies Hybridoma Bank; C651.6DbHN), NOTCH3 (Santa Cruz Biotechnology, sc-5593) and NOTCH4 (Santa Cruz Biotechnology, sc-8643) were diluted 1:1000.

### Cell isolation and culture

Primary human CTBs were isolated and cultured up to 36 hours as described (Hunkapiller and Fisher, 2008). For functional analyses, CTBs were cultured in medium containing either 10 μM L-685,458/0.1% DMSO or 0.1% DMSO. Mouse TS cells were cultured and differentiated using published methods (Maltepe et al., 2005).

### RT-qPCR

CTB and TS RNA samples were isolated using an RNeasy Plus kit (Qiagen). RNA concentration/quality was assessed using a Nanodrop spectrophotometer (Thermo-Scientific). cDNA libraries were prepared with 1 μg of RNA using the iScript kit (Biorad) and diluted 20-fold in water. SYBR green or Taqman RT-qPCR reactions were carried out in triplicate. Reaction specificity was confirmed by determining the melting curve of the products or by gel electrophoresis. Differences among target expression levels were estimated by the ΔΔCT method with normalization to *RN18S1* (SYBR green) and *GAPDH* (Taqman). The primer sequences are described in Table 1.

### TUNEL assays

CTBs were cultured in 1, 10 or 50 μM L-685,458 (Bachem), or DMSO alone. After 36 hours, the percentage of cells undergoing programmed cell death was estimated using an In Situ Cell Death Detection kit (Roche).

### Invasion assays

CTB invasion was assessed as described previously (Librach et al., 1991). Cells were plated with 10 μM L-685,458/0.1% DMSO or 0.1% DMSO and cultured for 36 hours.

### Mice

All protocols were approved by the UCSF Institutional Animal Care and Use Committee. For timed pregnancies, the day of vaginal plug detection was considered as E0.5. For assessment of placental *Tnr* activity, *Tnr* males [Jackson Laboratories; *Tg(Cp-EGFP)25Gaia/J*] were bred to wild-type FVB/NJ females (Jackson Laboratories). For *Notch2* deletion experiments, *Tpbpa-Cre* mice (Simmons et al., 2007) and *Notch2*$^{flox/flox}$ mice (McCright et al., 2006) were crossed. Genotyping primers are described in Table 1. Paraformaldehyde-fixed frozen placentas (E7.5-E15.5) were prepared and the embryos were genotyped.

### RNA in situ hybridization and KRT7 immunohistochemistry

Single probe RNA in situ hybridization was performed as previously described (Simmons et al., 2007). Notch family cDNAs were amplified from CTB RNA by using the RT-qPCR primers described in Table 1, which included either a 5′ T7 promoter sequence (TAATACGACTCACTATAGGG) or a 5′ T3 promoter sequence (AATTAACCCTCACTAAAGGG). Mouse cDNAs for *Prl2c2*, *Pcdh12* (Simmons et al., 2008), *Gcm1* (Basyuk et al., 1999), *Hand1* (Cross et al., 1995) and *Tpbpa* (Lescisin et al., 1988) have been described previously. The *Prl3b1* cDNA was provided by J. Rossant (The Hospital for Sick Children, Toronto, Canada) and the *Prl3d1* cDNA was provided by D. Linzer (Northwestern University, IL, ISA). cDNAs were used for digoxigenin probe synthesis according to the manufacturer's protocol

**Table 1. Primer sequences**

**qRT-PCR primers used in human and mouse experiments**

| Target gene | Forward primer 5′-3′ | Reverse primer 5′-3′ | Product size (bp) |
|---|---|---|---|
| *NOTCH1* | CTCACCTGGTGCAGACCCAG | GCACCTGTAGCTGGTGGCTG | 383 |
| *NOTCH2* | CAGTGTGCCACAGGTTTCACTG | GCATATACAGCGGAAACCATTCAC | 456 |
| *NOTCH3* | CGCCTGAGAATGATCACTGCTTC | TCACCCTTGGCCATGTTCTTC | 352 |
| *NOTCH4* | ATGACCTGCTCAACGGCTTC | GAAGATCAAGGCAGCTGGCTC | 237 |
| *JAG1* | GCTTGGATCTGTTGCTTGGTGAC | ACTTTCCAAGTCTCTGTTGTCCTG | 386 |
| *JAG2* | GCTATTTCGAGCTGCAGCTGAG | GCGGCAGGTAGAAGGAGTTG | 236 |
| *DLL1* | CTACACGGGCAGGAACTGCAG | CGCCTTCTTGTTGGTGTTCTTG | 441 |
| *DLL4* | CGGGTCATCTGCAGTGACAAC | AGTTGAGATCTTGGTCACAAAACAG | 348 |
| *RN18S1* | CGCCGCTAGAGGTGAAATTCT | CGAACCTCCGACTTTCGTTCT | 101 |
| *EFNB2* | Taqman Assay: Hs00187950_m1 | | 63 |
| *EPHB4* | Taqman Assay: Hs00174752_m1 | | 82 |
| *MMP9* | Taqman Assay: Hs00234579_m1 | | 54 |
| *GAPDH* | Taqman Assay: Hs02758991_g1 | | 93 |

**Genotyping primers**

| Target allele | Forward primer 5′-3′ | Reverse primer 5′-3′ | Product size (bp) |
|---|---|---|---|
| *Tnr* and *Tpbpa-Cre* | CACATGAAGCAGCACGACTT | ACTGGGTGCTCAGGTAGTGG | 385 |
| *Notch2*$^{flox/+}$ | TAGGAAGCAGCTCAGCTCACAG | ATAACGCTAAACGTGCACTGGAG | 200/161 |
| *Gt(ROSA)26Sor*$^{tm1Sor}$ | CGCCCGTTGCACCACAGATG | CCAGCTGGCGTAATAGCGAAG | 370 |

(Roche). *JAG1* hybridizations were followed by KRT7 immunolocalization as described previously (Winn et al., 2009). For double in situ hybridization, binding of the *Tnr* probe was detected by incubation with alkaline phosphatase-conjugated anti-digoxigenin followed by NBT/BCIP staining. Bound antibody was heat inactivated (65°C; 30 minutes) in maleic acid buffer/0.1% Tween-20. Then the slides were incubated in 0.1 M glycine (pH 2.2) for 30 minutes. Non-specific reactivity was blocked (Simmons et al., 2008) and fluorescein-labeled *Prl2c2* probe was detected following incubation with alkaline phosphatase-conjugated anti-fluorescein (Roche, 1:2500) and INT/BCIP staining. Sections were counterstained with nuclear Fast Red and mounted under 50% glycerol in PBS.

#### Evaluation of *Tpbpa-Cre* expression

*Tpbpa-Cre* females were bred with *Gt(ROSA)26Sor*$^{tm1Sor}$ males (Jackson Laboratories). Adult female F1 offspring were euthanized and ovarian and uterine tissues were embedded in OCT medium. Sections (5 μM) were fixed for 15 minutes in 0.1 M phosphate buffer (pH 7.3) supplemented with 5 mM EGTA, 2 mM $MgCl_2$ and 0.2% glutaraldehyde. Sections were washed in 0.1 M phosphate buffer (pH 7.3) supplemented with 2 mM $MgCl_2$. Staining was performed overnight at 37°C in 0.1 M phosphate buffer (pH 7.3) with 2 mM $MgCl_2$, 5 mM $K_3[Fe(CN)_6]$, 5 mM $K_4[Fe(CN)_6]•3H_2O$ and 5-Br-4-Cl-3-indolyl-β-D-galactoside (1 mg/ml) (Invitrogen). Sections were counterstained with nuclear Fast Red, dehydrated and mounted under Cytoseal 60 (Thermo-Scientific).

#### Vascular corrosion casting

*Notch2*$^{floxl+}$;*Tpbpa-Cre* females bred to *Notch2*$^{floxlflox}$;*Tpbpa-Cre* males were euthanized on day 10.5 or 14.5 of pregnancy and vascular corrosion casts were made as described previously (Adamson et al., 2002). Maternal canals were visualized by dissecting away venous and sinusoidal structures. The casts were photographed with a Leica MZ16 microscope, the diameter of individual canals was measured at the narrowest point, and the cross-sectional area was calculated and summed for each placenta.

#### Placental perfusion

Placental perfusion was estimated as described previously, with the exceptions noted (Plaks et al., 2010). At E12.5, *Notch2*$^{floxl+}$;*Tpbpa-Cre* females bred to *Notch2*$^{floxlflox}$;*Tpbpa-Cre* males were given tail vein injections of 200 μl (2 mg/ml) fluorescein-conjugated 70 kDa dextran (Invitrogen; D-1822). After 3 minutes, animals were euthanized. Placentas were dissected in ice-cold PBS, fixed in Carnoy's solution and embedded in paraffin wax. Sections (5 μm) were deparaffinized, rehydrated and mounted in Vectashield medium containing DAPI. Multiple sections from different areas of the placentas were imaged with a Leica DMI6000B microscope at 20× magnification and a photomontage of the entire sample was created. Average fluorescence intensity within the labyrinth was calculated using ImageJ software.

#### Statistics

Differences between means were assessed using either a paired two-tailed Student's *t*-test ($\alpha$=0.05) for RT-qPCR and CTB invasion experiments or assuming equal variance for the perfusion and casting experiments.

## RESULTS

### Human CTBs modulated expression of Notch molecules as they differentiated/invaded in vivo and in vitro

We used an immunolocalization approach to survey Notch family members at the human maternal-fetal interface (Fig. 1A). To validate antibody specificity, we assessed reactivity with endothelial cells, which served as internal positive controls (see Fig. S1A,B,F-K in the supplementary material), confirmed that antigens matched their expected molecular weight by immunoblotting (see Fig. S1C,D,E in the supplementary material), and/or correlated the findings with in vitro data obtained by an RT-qPCR approach (discussed in the next paragraph). The results showed that CTBs modulated the expression of Notch molecules in unique patterns as they invaded the uterus and the maternal arterioles that traverse this region. As to receptor localization, CTBs did not express NOTCH1 (see Fig. S1A,B in the supplementary material). Staining for NOTCH2 (Fig. 1B) was either absent or weak and sporadic in CTB progenitors that attached to the trophoblast basement membrane. However, NOTCH2 expression was dramatically upregulated in the CTB cell columns as invasion began. CTBs at all stages of differentiation stained for NOTCH3 (Fig. 1C,D). NOTCH4 immunoreactivity (Fig. 1E) was high in CTB progenitors and cell columns, and abruptly declined with deeper invasion, particularly as the cells approached spiral arterioles. Maternal and fetal cells stained for several Notch ligands. DLL1 was expressed (Fig. 1F) in maternal cells adjacent to CTBs in the interstitial and endovascular compartments. DLL4 staining (Fig. 1G) was not detected in CTB progenitors but increased as the cells entered the columns. However, DLL4 immunoreactivity was rapidly lost as CTBs invaded the uterine wall, although small fields of immunopositive cells were occasionally observed in the deeper regions. JAG1 expression (Fig. 1H,I), which was absent in early stages of CTB differentiation/invasion, was significantly upregulated in CTBs that associated with the maternal spiral arterioles. CTBs did not express JAG2 (not shown). The staining patterns for individual family members and a diagrammatic summary of the results are presented in Fig. S2 in the supplementary material. Together, these data show that CTBs dramatically altered their expression of Notch receptors and ligands as they differentiated/invaded.

Next, we used a RT-qPCR approach to assess Notch family mRNA expression patterns in an in vitro system (Fig. 2A): CTBs grown on Matrigel model interstitial differentiation/invasion in vivo (Librach et al., 1991; Zhou et al., 1997). In general, the results recapitulated the immunoanalyses. *NOTCH2* mRNA levels peaked at 3 hours, *NOTCH3* mRNA levels remained constant and *NOTCH4* expression quickly declined with differentiation. *DLL4* mRNA levels increased with differentiation. However, we repeatedly failed to detect *JAG1* expression at either mRNA or protein levels under a variety of culture conditions we used to simulate the uterine vascular environment, e.g. EC, decidual cell or explanted spiral arteriole co-culture, as well as physiological hypoxia, shear stress or high serum concentrations (data not shown). This was consistent with our conclusion that this culture model does not replicate the terminal stages of CTB endovascular invasion, e.g. upregulation of NCAM1 (Blankenship and King, 1996). Thus, the results of these experiments showed that this culture model is useful for studying Notch functions during the interstitial phases of differentiation/invasion but not during the final stages of endovascular remodeling.

### Notch signaling regulated CTB invasion and expression of *EFNB2*, an arterial marker

CTBs were plated with L-685,458, a chemical inhibitor of γ-secretase proteolytic activity, which is required for Notch protein activation. However, γ-secretase is involved in other signaling pathways (Hass et al., 2009) and L-685,458 also inhibits signal peptide peptidases (Weihofen et al., 2003). First, we determined whether L-685,458, at concentrations that are typically used to inhibit Notch signaling (Williams et al., 2006), had toxic effects. After 36 hours, the percentage of CTBs undergoing programmed cell death was assessed by using the terminal deoxynucleotidyltransferase-mediated dUTP-biotin nick end labeling method (TUNEL). Virtually no apoptosis was detected at L-685,458 concentrations up to 10 μM

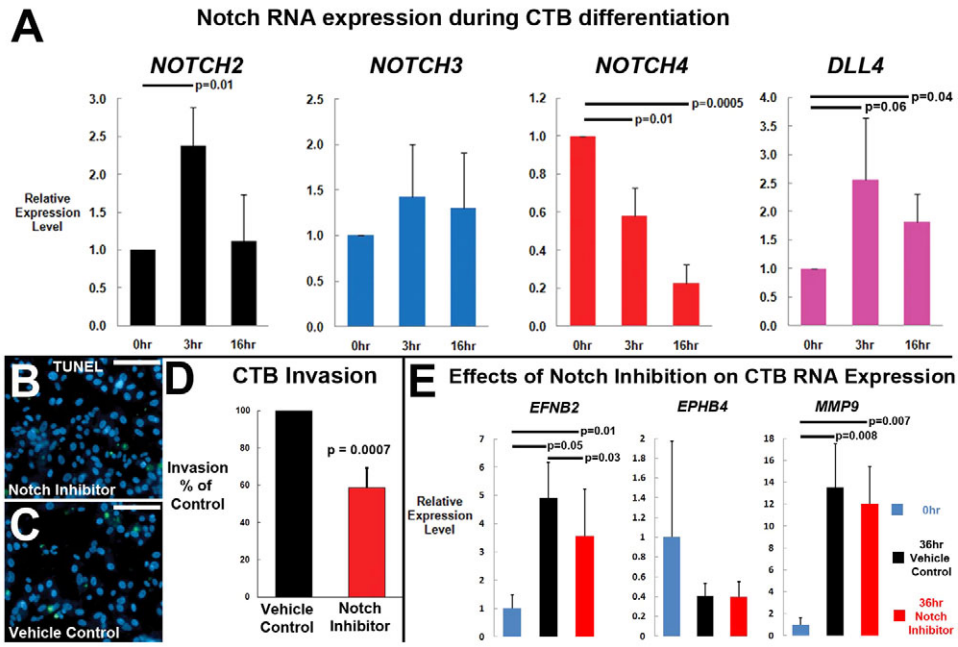


**Fig. 2. Notch inhibition reduced CTB invasion and *EFNB2* expression in vitro.** (**A**) Expression of Notch family member RNA in CTBs was quantified as they differentiated in culture over a 16-hour period. *NOTCH2* and *DLL4* expression increased, *NOTCH3* expression remained constant, and *NOTCH4* expression decreased. (**B**,**C**) The level of CTB apoptosis, which was assessed using the TUNEL method, was negligible in experimental cultures that contained the Notch inhibitor L-685,458 (10 μM) (B) and in control conditions (C). TUNEL-positive apoptotic cells were visualized with FITC (green) and cell nuclei were stained with DAPI (blue). Scale bars: 100 μm. (**D**) Notch inhibition reduced CTB invasion through Matrigel by 40% ($n$=10). (**E**) CTB *EFNB2*, *EPHB4* and *MMP9* RNA expression was measured by Taqman at 0 hours and after the cells had fully differentiated in culture (36 hours) with or without the Notch inhibitor. Compared with controls, CTBs cultured with L-685,458 expressed lower levels of *EFNB2*. *GAPDH* served as a loading control. Data are represented as mean+s.d.

(Fig. 2B,C and data not shown). Therefore, this inhibitor concentration was subsequently employed. Next, we assessed the effects of inhibiting Notch activation on CTB invasion. L-685,458 significantly decreased invasion (Fig. 2D), evidence that Notch family members play a role in this process. Finally, we asked whether Notch inhibition affected the ability of the cells to upregulate the expression of markers of arterial ECs as they differentiated/invaded in culture. These experiments exploited our observation that, during this process, CTBs downregulate *EPHB4* and upregulate *EFNB2*, markers of venous and arterial ECs, respectively (Red-Horse et al., 2005). Under control conditions, we observed robust upregulation of *EFNB2* mRNA after 36 hours (Fig. 2E). In the presence of L-685,458, *EFNB2* expression was blunted by 27% ($P$=0.025), as measured by Taqman RT-qPCR. By contrast, L-685,458 had no effect on *EPHB4* or *MMP9*, which is required for CTB invasion (Librach et al., 1991). Together, these results supported a model in which Notch activity promoted CTB differentiation/invasion and acquisition of an arterial EC-like phenotype. Because cultured CTBs failed to replicate the terminal stages of CTB endovascular differentiation, we used mouse models to study the role of Notch in this process.

## Placental Notch activity was largely confined to the mouse ectoplacental cone and endovascular trophoblasts

As the co-expression of Notch ligands and receptors does not necessarily correlate with function, independent methods are required to estimate Notch activity. However, few tools have been developed for use in human cells. Accordingly, we used the mouse transgenic Notch reporter (*Tnr*) line that expresses *Gfp* under the control of a Notch responsive promoter (Duncan et al., 2005) to assess Notch activity during development of the placenta. *Tnr* offspring and placentas were generated from timed matings between wild-type females and males harboring the *Tnr* transgene. Notch activity was first observed at E7.5 in a few rare cells at the leading edge of the ectoplacental cone (EPC), the primary source of invasive trophoblasts (data not shown). By E8.5, Notch activity was detected in association with many more EPC cells, particularly in the outer layers that were in contact with the uterus (Fig. 3A). Between E8.5 and E10.5, a subset of TGCs at the periphery of the implantation site acquired Notch activity, which was also evident in a growing population of trophoblast cells within the junctional zone (see Fig. S3A-C in the supplementary material), a region analogous to the maternal-fetal interface in humans. By E14.5 (Fig. 3B,C), the highest Notch activity was restricted to trophoblasts that were associated with maternal spiral arterioles with lower levels observed in the spongiotrophoblast region and in association with other cells that were sparsely distributed throughout the labyrinth. Placentas without the *Tnr* allele lacked *Gfp* signal (see Fig. S3D in the supplementary material). In mice, spiral artery-associated TGCs (SpA-TGCs) and GlyTCs carry out endovascular invasion, suggesting that Notch activity was dramatically increased in these cells. To confirm this theory, we quantified *Tnr* and trophoblast lineage marker co-expression by RNA in situ hybridization. Because of differences in probe strength, we performed double hybridizations for *Tnr* (Notch activity) and the TGC marker *Prl2c2*

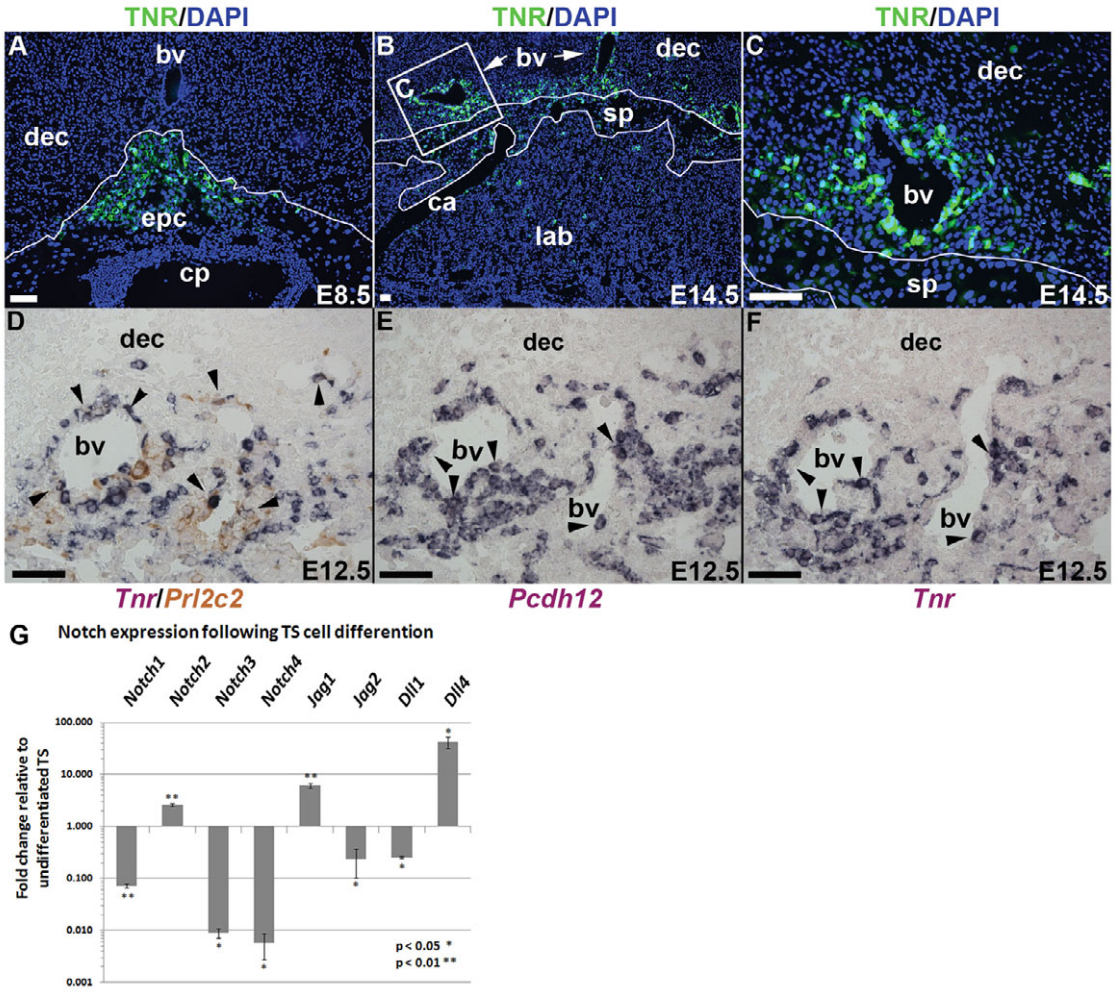


**Fig. 3. Notch activity was highest in invasive GlyTCs and TGCs that associated with uterine spiral arterioles.** (**A-C**) Tissue sections from the placentas of *Tnr* mice enabled assessment of Notch activity (green) across gestation. Nuclei were stained with DAPI (blue). (A) At E8.5 (*n*=5), Notch activity was observed in the ectoplacental cone (epc). (B,C) At E14.5 (*n*=9), Notch activity was highest in invasive trophoblast cells surrounding maternal blood vessels (bv). (**D-F**) Double (D) or single (E,F) in situ hybridization was performed on sections of E12.5 *Tnr* placentas (*n*=13) to detect Notch activity (purple) and expression of the mouse trophoblast lineage-specific markers *Prl2c2* (TGCs; brown) or *Pcdh12* (GlyTCs; purple). Nuclei were stained with nuclear Fast Red. Arrowheads indicate double-positive cells. Approximately half of spiral artery-associated (D) TGCs and (E) GlyTCs had (F) Notch activity. Scale bars: 100 μm. ca, canal; cp, chorionic plate; dec, decidua; lab, labyrinth; sp, spongiotrophoblast. (**G**) Mouse trophoblast stem cells regulated the expression of Notch family members as they differentiated in vitro. Notch RNA expression levels were normalized to *Rn18s*. *Notch2*, *Jag1* and *Dll4* were upregulated with trophoblast differentiation; levels of all other family members declined. Data are represented as mean±s.d.

(Fig. 3D), and analyzed serial sections for *Tnr* (Fig. 3E) and the GlyTC marker *Pcdh12* (Fig. 3F) (*n*=13). *Prl2c2*-positive SpA-TGCs (48±8%) and approximately half of *Pcdh12*-positive endovascular GlyTCs had Notch activity. Accordingly, we profiled mouse TB expression of Notch family members with the goal of focusing subsequent studies on receptors that could mediate differentiation/invasion. We compared RNA levels in TS cells, which are known to express all components of the Notch pathway (Cormier et al., 2004), to their differentiated progeny, grown under normoxic conditions that produce primarily TGCs (Fig. 3G). Very similar to the patterns observed in human CTBs in vivo, only *Notch2*, *Jag1* and *Dll4* expression increased with differentiation, whereas *Notch1*, *Notch3*, *Notch4*, *Jag2* and *Dll1* expression declined. Taken together, these findings bolstered the conclusions of the in vitro human experiments that implicated Notch activity as a driver of CTB endovascular invasion.

## *Notch2* deletion in invasive trophoblast lineages led to litter-wide lethality in proportion to the number of mutant offspring

To investigate Notch function with regard to trophoblast invasion of spiral arterioles, we designed a strategy for conditional deletion of *Notch2* in the invasive trophoblast lineages, which includes all SpA-TGCs and GlyTCs. Briefly, we bred mice harboring floxed alleles of *Notch2* (*Notch2*$^{flox}$) (McCright et al., 2006) to *Tpbpa-Cre* mice (Simmons et al., 2007) in which *Cre* recombinase is specifically expressed by EPC cells that later give rise to all GlyTCs, SpA-TGCs and spongiotrophoblasts. Following their differentiation from EPC precursors, spongiotrophoblasts normally maintain *Tpbpa* expression, which GlyTCs and SpA-TGCs lose. To confirm the expected expression pattern, we performed serial RNA in situ hybridization for both *Tpbpa* and *Gfp*, which is also a component of the *Tpbpa-Cre* construct. *Gfp* expression by

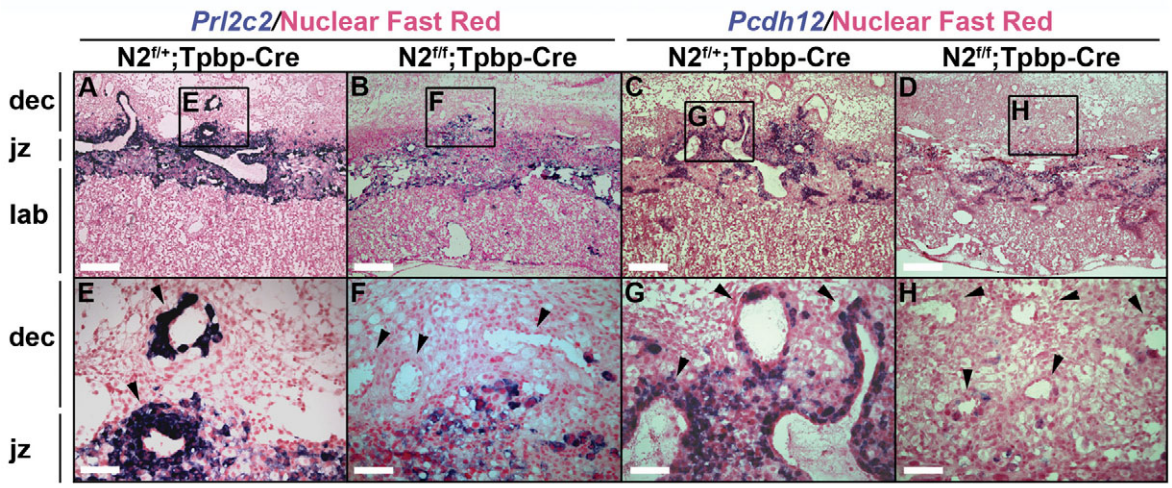


**Fig. 4. Conditional deletion of *Notch2* in invasive trophoblasts reduced TGC and GlyTC invasion of spiral arterioles.** (**A-H**) In situ hybridization was performed on tissue sections of E12.5 *Notch2*$^{floxl+}$;*Tpbpa-Cre* and *Notch2*$^{floxlflox}$;*Tpbpa-Cre* placentas for the TGC marker *Prl2c2* (A,B, magnified in E,F, respectively) and the GlyTC marker *Pcdh12* (C,D, magnified in G,H, respectively). Hybridization was visualized by NBT/BCIP staining (purple). Nuclei were stained with nuclear Fast Red. The decidua (dec), junctional zone (jz) and labyrinth (lab) are shown. In *Notch2*$^{floxlflox}$;*Tpbpa-Cre* mice, very few TGCs and GlyTCs invaded spiral arterioles (arrowheads). Scale bars: 400 μm in A-D; 100 μm in E-H.

spongiotrophoblasts typically occurred in nearly all cells at E9.5 (see Fig. S4A,B in the supplementary material) and in the majority of cells at E12.5 (see Fig. S4C,D in the supplementary material), evidence that the construct was expressed in the desired location.

Accordingly, we generated *Notch2*$^{floxl+}$;*Tpbpa-Cre* (heterozygote) and *Notch2*$^{floxlflox}$;*Tpbpa-Cre* (mutant) embryos and offspring by breeding *Notch2*$^{floxlflox}$ and *Tpbpa-Cre* founders. In preliminary crosses, *Notch2*$^{floxlflox}$;*Tpbpa-Cre* offspring were born that were used for breeding purposes. Given that complete embryonic loss of *Notch2* results in lethality by E11.5 (Hamada et al., 1999), we focused our analysis on this developmental window. First, we surveyed resorption rates in litters generated from different combinations of *Notch2*$^{floxl+}$;*Tpbpa-Cre* or *Notch2*$^{floxlflox}$;*Tpbpa-Cre* parents, designed to produce 25%, 50% or 100% *Notch2*$^{floxlflox}$;*Tpbpa-Cre* progeny (see Table S1 in the supplementary material). In litters bred from *Notch2*$^{floxl+}$;*Tpbpa-Cre* animals, only one resorption was observed among the 39 implantation sites (2.6%) examined between E10.5-E12.5. Breeding of *Notch2*$^{floxl+}$;*Tpbpa-Cre* and *Notch2*$^{floxlflox}$;*Tpbpa-Cre* animals produced litters with many more resorptions. Loses, which were observed as early as E9.5, increased to a maximal frequency of 29% by E11.5. A similar temporal pattern was observed in *Notch2*$^{floxlflox}$;*Tpbpa-Cre* matings, but the resorption rate increased to 54%. Maternal factors did not contribute to increases in embryonic lethality, as crosses of *Notch2*$^{floxl+}$;*Tpbpa-Cre* females to *Notch2*$^{floxlflox}$;*Tpbpa-Cre* males and reciprocal crosses of *Notch2*$^{floxlflox}$;*Tpbpa-Cre* females to *Notch2*$^{floxl+}$;*Tpbpa-Cre* males exhibited similar rates of resorption (see Table S2 in the supplementary material). Next, we correlated embryonic genotype with resorption/survival (see Table S3 in the supplementary material). Surprisingly, in *Notch2*$^{floxl+}$;*Tpbpa-Cre* × *Notch2*$^{floxlflox}$;*Tpbpa-Cre* matings, resorptions involved equal numbers of *Notch2*$^{floxl+}$;*Tpbpa-Cre* and *Notch2*$^{floxlflox}$;*Tpbpa-Cre* embryos. This conclusion was substantiated by the fact that the surviving offspring had the same genetic distribution. Consistent with this observation, we did not note any differences in embryonic or placental weight between *Notch2*$^{floxl+}$;*Tpbpa-Cre* and *Notch2*$^{floxlflox}$;*Tpbpa-Cre* offspring (see Table S4 in the supplementary material). Taken together, these results suggest that embryonic lethality correlated with the presence of *Notch2*$^{floxlflox}$;*Tpbpa-Cre* embryos rather than the genotype of individual fetuses.

In initial breeding experiments, we noted that *Notch2*$^{floxlflox}$;*Tpbpa-Cre* mothers had significantly fewer implantation sites than *Notch2*$^{floxl+}$;*Tpbpa-Cre* mothers (5.7±2.8 versus 7.5±2.8; $P$=0.03). This result was independent of embryonic genotype, as the implantation rate was identical in *Notch2*$^{floxlflox}$;*Tpbpa-Cre* females bred to *Notch2*$^{floxl+}$;*Tpbpa-Cre* or *Notch2*$^{floxlflox}$;*Tpbpa-Cre* males. In searching for a possible explanation, we discovered that the *Notch2*$^{floxlflox}$;*Tpbpa-Cre* females exhibited severe ovarian defects, including hemorrhagic and cystic follicles, which were not observed in *Notch2*$^{floxl+}$;*Tpbpa-Cre* females (see Fig. S5A in the supplementary material). These observations suggested that the *Tpbpa-Cre* transgene might also have ovarian expression. To address this possibility, we bred *Tpbpa-Cre* females to males of the Cre reporter strain *Gt(ROSA)26Sor*$^{tm1Sor}$, which has a *ROSA26-lox-stop-lox-lacZ* sequence, and examined *Gt(ROSA)26Sor*$^{tm1Sor}$;*Tpbpa-Cre* embryos/offspring for β-galactosidase activity (i.e. evidence of *Tpbpa-Cre* expression). In placentas, we observed β-galactosidase activity in spongiotrophoblasts, TGC, and GlyTCs as previously reported (Simmons et al., 2007). In the adult ovaries, we observed β-galactosidase activity in the granulosa cells (see Fig. S5B in the supplementary material). We also noted infrequent *Rosa26-lacZ* recombination events in a small percentage of cells (~1-5%) in other organs, including the uterus (see Fig. S5C in the supplementary material). We performed RNA in situ hybridization for *Tpbpa* to assess possible ovarian expression. In the absence of signal (see Fig. S5D in the supplementary material), the ovarian phenotype was attributable to nonspecific promoter activity. Thus, to avoid possible confounding ovarian effects in *Notch2*$^{floxlflox}$;*Tpbpa-Cre* mothers, all the data used to compare *Notch2*$^{floxl+}$;*Tpbpa-Cre* and *Notch2*$^{floxlflox}$;*Tpbpa-Cre* offspring were generated from experiments using *Notch2*$^{floxl+}$;*Tpbpa-Cre* mothers, and comparisons were made between offspring of the same litter. Additionally, to ensure that *Notch2*$^{floxl+}$;*Tpbpa-Cre*

mothers ($n$=8) had normal reproductive function, we confirmed that they exhibited normal birth rates in comparison with *Notch2*$^{floxlflox}$ mothers (wild type; $n$=7) (8.38±1.1 versus 8.44±2.6; $P$=0.95).

### In the absence of *Notch2*, TGCs and GlyTCs failed to invade maternal spiral arterioles, which was associated with reduced canal size and placental perfusion

To assess whether trophoblast differentiation/invasion failed in *Notch2*$^{floxlflox}$;*Tpbpa-Cre* placentas, we used RNA in situ hybridization to survey lineage-specific markers. No overt differences were observed at E9.5 or E12.5 between *Notch2*$^{floxl+}$, *Notch2*$^{floxl+}$;*Tpbpa-Cre* and *Notch2*$^{floxlflox}$;*Tpbpa-Cre* placentas with regard to the presence/absence of markers of labyrinthian trophoblast cell types (*Gcm1*, *Hand1*), spongiotrophoblasts (*Tpbpa*), TGCs (*Prl3d1*, *Prl3b1* and *Prl2c2*) or GlyTCs (*Pcdh12*) (see Fig. S6 in the supplementary material and data not shown). However, although TGCs and GlyTCs in *Notch2*$^{floxl+}$;*Tpbpa-Cre* placentas robustly invaded maternal spiral arterioles at E12.5 (10/11 placentas examined) (Fig. 4A,C; enlarged in Fig. 4E,G, respectively), this process failed in the large majority of the *Notch2*$^{floxlflox}$;*Tpbpa-Cre* placentas (7/9 placentas examined) (Fig. 4B,D; enlarged in Fig. 4F,H, respectively). To rule out possible differences in marker expression levels in *Notch2*$^{floxlflox}$;*Tpbpa-Cre* placentas, we confirmed these results by immunostaining with the Tromo-1 antibody (see Fig. S7 in the supplementary material), which reacts with a cytokeratin that is expressed by all trophoblast populations (Amarante-Paffaro et al., 2011).

Accordingly, we explored the functional consequences of these observations. Specifically, we looked for abnormalities in the structure of the trophoblast-lined canals that transport maternal blood to the placenta. To obtain an integrated view of the anatomical basis of placental perfusion, we prepared vascular corrosion casts of the maternal circulation at E10.5 and E14.5 (Fig. 5). Overall, the branching patterns in *Notch2*$^{floxlflox}$;*Tpbpa-Cre* and *Notch2*$^{floxl+}$;*Tpbpa-Cre* placentas were similar; maternal blood entered the decidua through a tortuous network of ~8-12 interconnected spiral arterioles that converged into ~1-4 canals at the junctional zone boundary before spreading into a sinusoidal network at the base of the labyrinth. Given the complexity of the spiral artery network, we focused our analysis on the terminal regions of the canals. At E10.5, the canals in *Notch2*$^{floxl+}$;*Tpbpa-Cre* placentas (Fig. 5A; magnified in Fig. 5C) were larger than those in *Notch2*$^{floxlflox}$;*Tpbpa-Cre* placentas (Fig. 5B; magnified in Fig. 5D). We noted similar differences between *Notch2*$^{floxl+}$;*Tpbpa-Cre* (Fig. 5E; magnified in Fig. 5G) and *Notch2*$^{floxlflox}$;*Tpbpa-Cre* animals (Fig. 5F; magnified in Fig. 5H) at E14.5. These results were quantified by translating the estimated vessel diameters into cross-sectional areas (Fig. 5I). The results showed significant decreases in *Notch2*$^{floxlflox}$;*Tpbpa-Cre* placentas at E10.5 (40%) and E14.5 (34%). No significant differences were observed between *Notch2*$^{floxl+}$;*Tpbpa-Cre* ($n$=14) and *Notch2*$^{floxlflox}$;*Tpbpa-Cre* ($n$=11) animals in the average number of canals per placenta (3.2±1.2 versus 2.9±1.0; $P$=0.51).

The reduced canal size in *Notch2*$^{floxlflox}$;*Tpbpa-Cre* placentas suggested that placental perfusion might be compromised. To test this theory, we estimated possible differences by injecting a 70 kDa fluorescein-conjugated dextran via the tail vein and measuring its short-term accumulation within the labyrinth at E12.5 (Plaks et al., 2010). Analysis of placental tissue sections from *Notch2*$^{floxl+}$;*Tpbpa-Cre* animals (Fig. 6A,B) when compared with their

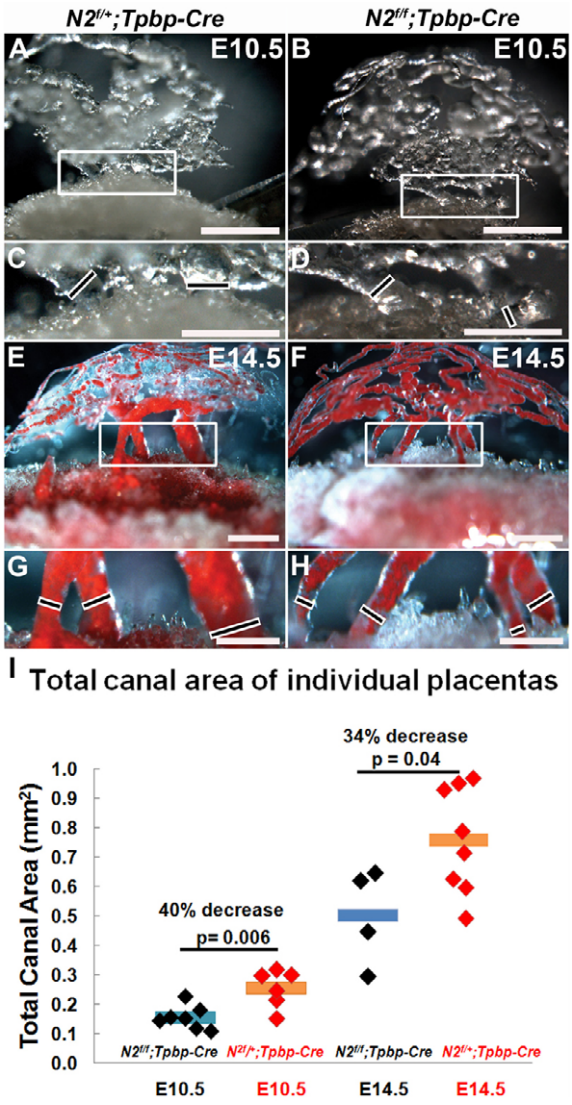


**Fig. 5. The trophoblast-lined vascular canals that supply blood to the placenta were smaller in *Notch2*$^{floxlflox}$;*Tpbpa-Cre* mice.** (**A-H**) Vascular corrosion casts of the maternal blood spaces of the placenta were prepared at E10.5 and E14.5. In placentas of *Notch2*$^{floxl+}$;*Tpbpa-Cre* and *Notch2*$^{floxlflox}$;*Tpbpa-Cre* offspring, a complex array of maternal spiral arterioles converged into several large canals before branching into the labyrinthian sinusoids. At E10.5, the canals in *Notch2*$^{floxl+}$;*Tpbpa-Cre* placentas (A; enlarged in C) ($n$=6) were larger than those in *Notch2*$^{floxlflox}$;*Tpbpa-Cre* placentas (B; enlarged in D) ($n$=7). We noted similar differences between *Notch2*$^{floxl+}$;*Tpbpa-Cre* (E; enlarged in G) ($n$=8) and *Notch2*$^{floxlflox}$;*Tpbpa-Cre* animals (F; enlarged in H) ($n$=4) at E14.5. Scale bars: 1 mm in A,B,E,F; 500 μm in C,D,G,H. (**I**) The vessel diameter was used to calculate the cross-sectional areas of the canals. At E10.5 and E14.5, vessels in *Notch2*$^{floxlflox}$;*Tpbpa-Cre* placentas were 40% and 34% smaller, respectively, when compared with *Notch2*$^{floxl+}$;*Tpbpa-Cre* animals. Group means are represented as solid bars.

*Notch2*$^{floxlflox}$;*Tpbpa-Cre* counterparts (Fig. 6C,D) revealed increased fluorescence intensity. Although we did not observe differences between the two groups in the relative size of the placental labyrinth or its vascular spaces, quantification of the total labyrinthian-FITC signal showed that *Notch2*$^{floxlflox}$;*Tpbpa-Cre* placentas accumulated 23% less fluorescein-conjugated dextran (Fig. 6E). Together, the

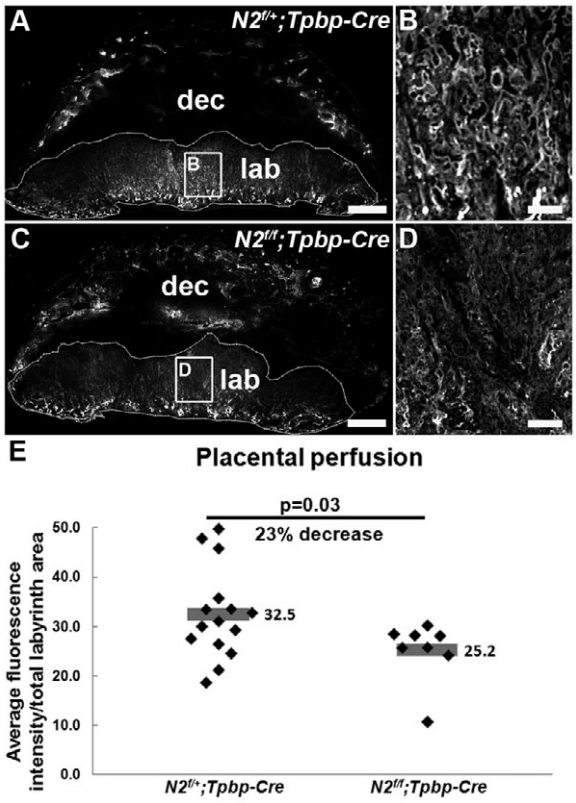


**Fig. 6. Placental perfusion was compromised in *Notch2*$^{floxlflox}$;*Tpbpa-Cre* animals.** (**A-D**) To approximate placental perfusion, animals were injected i.v. with fluorescein-conjugated dextran and tissue sections of the labyrinth (lab) were analyzed for the short-term (3-minute) accumulation of this tracer. The FITC signal, which appeared to be stronger in the labyrinth (outlined) of *Notch2*$^{floxl+}$;*Tpbpa-Cre* placentas (A; enlarged in B) ($n$=15) when compared with *Notch2*$^{floxlflox}$;*Tpbpa-Cre* littermates (C; enlarged in D) ($n$=8), was quantified by using ImageJ (**E**). Placental perfusion was reduced by ~23% in *Notch2*$^{floxlflox}$;*Tpbpa-Cre* placentas. Group means are represented as solid bars. Scale bars: 1 mm in A,C; 200 μm in B,D. dec, decidua.

results of the marker analyses, vascular corrosion casting and placental perfusion experiments supported a possible causal relationship between *Notch2*-directed trophoblast invasion of spiral arteries and corresponding increases in placental perfusion.

### In PE, CTBs that associated with spiral arterioles failed to express JAG1

Based on the mouse data, we tested the hypothesis that the faulty CTB differentiation/invasion observed in PE is associated with alterations in the expression of Notch molecules. As we previously described, pre-term labor (PTL) cases, which we used as controls, were associated with normal levels of CTB interstitial, perivascular and endovascular invasion (Zhou et al., 2007) (Fig. 7A-C). In addition, CTB differentiation in PTL is normal, as are gene expression patterns in the basal plate (Winn et al., 2009). By contrast, CTB invasion was variably reduced in severe pre-eclampsia (SPE), and in the hemolysis, elevated liver enzymes and low platelets (HELLP) syndrome. In some instances, CTB invasion failed altogether. In others, CTBs were either confined to perivascular spaces (Fig. 7D), exhibited limited endovascular invasion (Fig. 7E) or transformed maternal arteries as in normal pregnancy (Fig. 7F). To assess the expression of Notch family members, we used immunolocalization and RNA in situ hybridization approaches. We failed to detect any differences between cases and controls in CTB *NOTCH2-4* and *DLL4* expression patterns and staining intensities (data not shown). Similar to our observations in second trimester biopsies, the majority of perivascular and endovascular CTBs exhibited robust *JAG1* mRNA expression in PTL samples (Fig. 7A-C). However, a CTB *JAG1* signal was absent in many vessels from PE cases (Fig. 7D-F) regardless of the extent of vascular remodeling. We confirmed these findings at the protein level (Fig. 7G,H). We calculated the percentage of *JAG1*-positive CTB-modified vessels in individual PTL and PE cases (Fig. 7I and see Table S5 in the supplementary material). All the modified vessels in each of six PTL control cases contained *JAG1*-positive CTBs. This fraction was reduced to 53% in ten SPE cases and to 26% in three HELLP cases. Taken together, the correlation between reduced *JAG1* expression and failed vascular remodeling in PE suggests that Notch signaling plays an important functional role in remodeling of human spiral arterioles.

## DISCUSSION

Through their aggressive invasion/remodeling of uterine vessels, CTBs incorporate the placenta into the maternal circulation. As this component of placentation fails in PE, the mechanisms involved are of great interest. The first evidence that Notch might regulate CTB differentiation/invasion came from experiments in which we profiled Notch expression in tissue sections of the human placenta and in CTBs that were differentiating in vitro. Notably, multiple Notch pathway components were similarly expressed by CTBs in both contexts and were precisely modulated during specific stages of the invasion process. Functional inhibition in cultured CTBs confirmed that Notch signaling influenced interstitial CTB invasion and *EFNB2* expression. To understand Notch functions during endovascular invasion, we used mouse models to demonstrate that the endovascular trophoblast populations possessed the highest levels of Notch activity and that Notch expression patterns were similar in both species. As *Notch2* was the only receptor upregulated during mouse trophoblast invasion, we targeted this molecule for deletion in the invasive trophoblast lineages. Unexpectedly, *Notch2*$^{floxl+}$;*Tpbpa-Cre* and *Notch2*$^{floxlflox}$;*Tpbpa-Cre* embryos were lost in proportion to the number of *Notch2*$^{floxlflox}$;*Tpbpa-Cre* offspring, suggesting that failures of individual feto-placental units had litter-wide effects. *Notch2* proved to be a crucial determinant of endovascular invasion; TGCs and GlyTCs from *Notch2*$^{floxlflox}$;*Tpbpa-Cre* placentas failed to invade maternal spiral arterioles. Furthermore, failed endovascular invasion was associated with decreased canal size in *Notch2*$^{floxlflox}$;*Tpbpa-Cre* animals, a likely cause of the observed decline in placental perfusion. As Notch signaling was required for endovascular invasion in the mouse, we investigated the expression of family members in PE, which is associated with failures in this process. The results showed that artery-associated CTBs often lacked JAG1 expression. To our knowledge, JAG1 is the only marker that distinguishes between endovascular CTBs in normal pregnancies and those complicated by PE.

Notch functions in other cellular contexts offer unique insights into how these signaling pathways specify trophoblast identity and regulate endovascular invasion. *Notch2* is the only receptor that has not been associated with arterial identity (Villa et al., 2001). In developing vascular beds, Notch signaling in EC progenitors promotes their assumption of arterial identity, which is

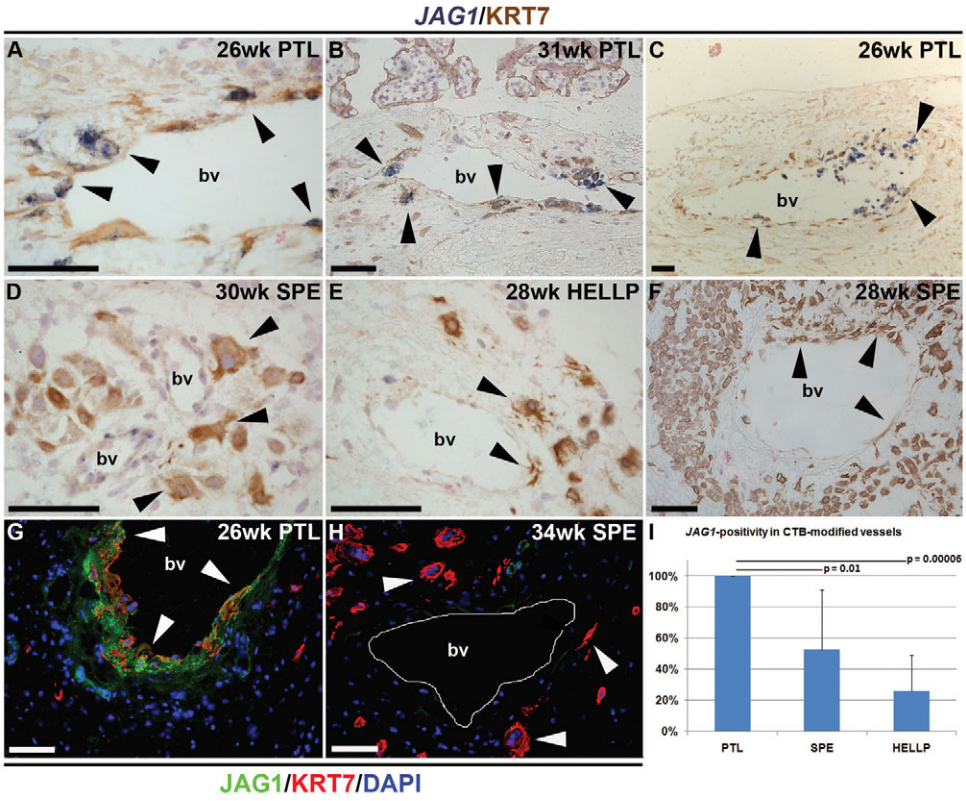


**Fig. 7. In PE, endovascular and perivascular CTBs failed to express JAG1.** (**A-F**) *JAG1* in situ hybridization (purple) and KRT7 immunolocalization (brown) were performed on tissue sections of basal plate biopsies from PTL and PE cases (SPE and HELLP). (A-C) In PTL, endovascular and perivascular CTBs (arrowheads) expressed *JAG1*. (D-F) In PE, fewer vessels were modified and many of the associated CTBs lacked *JAG1* expression. (**G**,**H**) Double indirect immunolocalization of JAG1 and KRT7 confirmed these results at the protein level. Nuclei were stained with DAPI. (**I**) Tissue sections from six PTL, ten SPE and three HELLP cases were scored for the percentage of modified maternal vessels that contained JAG1-positive CTBs. The mean decreased to 53% in SPE and to 26% in HELLP. Individual results are reported in Table S5 in the supplementary material. Data are represented as mean+s.d. Scale bars: 100 μm. bv, blood vessel.

characterized by *Efnb2* expression in the absence *Ephb4*. The converse is observed in venous endothelium, helping to organize arteriovenous boundaries through repulsive interactions generated through bi-directional signaling between adjacent cells. We have previously demonstrated that *EFNB2/EPHB4* play similar roles in directing CTB invasion away from the placenta and toward uterine spiral arterioles (Red-Horse et al., 2005). Here, we showed that Notch plays an upstream role in regulating CTB *EFNB2* expression.

The striking upregulation of JAG1 expression and Notch activity in the endovascular trophoblast populations suggests that CTBs experience physiological cues that promote Notch signaling and subsequent *EFNB2*-dependent endovascular invasion. Shear stress and cyclic strain, which are high in uterine spiral arterioles and low in uterine veins during pregnancy, offer possible explanations of how Notch signaling is initiated in the arteries. In ECs, these forces rapidly enhance Notch receptor cleavage/activation, increase expression of Notch receptors and ligands, and promote Notch-dependent *EFNB2* upregulation (Masumura et al., 2009; Morrow et al., 2007; Wang et al., 2007). Interestingly, ligand endocytosis potentiates cleavage and activation of Notch receptors, leading several groups to propose that mechanical forces expose the S2 cleavage site within the Notch receptor (Kopan and Ilagan, 2009). Thus, it is possible that cyclic strain and shear stress experienced by CTBs near spiral arterioles provides a mechanical force that potentiates Notch activation, JAG1 upregulation and EFNB2-dependent signaling. However, our attempts to modulate CTB expression of Notch family members with shear stress were unsuccessful. Likewise, CTB co-culture with ECs or decidual cells, and in a low oxygen tension environment failed to upregulate JAG1 expression. Thus, it is likely that a complex interplay among cell types and physiological factors is required.

*Notch2* function is required for mouse placental development (Hamada et al., 2007). Tetraploid complementation, in which *Notch2*-deficient embryos were provided with wild-type placentas, revealed placental insufficiency as the primary cause of lethality. *Notch2*$^{-/-}$ animals exhibited dramatic reductions in maternal blood spaces within the placental labyrinth without obvious defects in the differentiation of labyrinthian trophoblasts, spongiotrophoblasts or TGCs. However, the mechanism of placental insufficiency remained to be elucidated. Our observation that Notch activity was highest in the endovascular trophoblast populations suggested that this remodeling process played an important role in determining the *Notch2*$^{-/-}$ placental phenotype. We addressed this possibility by specifically eliminating *Notch2* in this population. These experiments revealed similar phenotypes in terms of the timing of embryo loss and reduced accumulation of maternal blood in the labyrinth, but differed in that we did not observe changes in the size of the maternal sinusoidal spaces. Rather, our study uniquely identified deficits in endovascular invasion and decreases in the

size of canals that supply blood to the labyrinth. The disparate phenotypic outcomes of the two gene deletion strategies may highlight unique functions of endovascular and labyrinthian *Notch2* activity; labyrinthian cells appear to play a distinct role in organizing the sinusoidal blood spaces, whereas endovascular trophoblasts coordinate maternal increases in blood supply.

Interestingly, disrupting perfusion of individual placentas had litter-wide effects on pregnancy outcome. The frequency of fetal resorption correlated with the percentage of *Notch2*$^{floxlflox}$;*Tpbpa-Cre* offspring in the litter. Unexpectedly, fetal loss was equally distributed among littermates regardless of genotype. As mice with *Notch2* haploinsufficiency are viable (Witt et al., 2003), these results suggested that reducing perfusion in *Notch2*$^{floxlflox}$;*Tpbpa-Cre* placentas had negative effects on the survival of both *Notch2*$^{floxl+}$;*Tpbpa-Cre* and *Notch2*$^{floxlflox}$;*Tpbpa-Cre* animals. Although the mechanism(s) is unknown, it is well established that endovascular invasion produces local decreases in vascular resistance of the arteries that supply each fetus. Conversely, failed vascular transformation is associated with local increases in vascular tone that drive parallel systemic changes. These effects could account for our finding. This theory is supported by observations made in the reduced utero-placental perfusion model (RUPP) in which the uterine blood flow of pregnant rats is surgically reduced. RUPP increases sensitivity to vasoactive factors at both local and systemic levels, which results in hypertension (Anderson et al., 2005; Crews et al., 2000). These findings were further substantiated by a recent study of placental gene expression in the Norway Brown rat (Goyal et al., 2010), a strain that exhibits significantly decreased trophoblast vascular invasion. Compared with control strains, the placentas of these animals secrete increased levels of vasoconstrictive factors and decreased amounts of vasodilators. Additionally, they have a much higher rate of fetal loss. Taken together, these studies may explain how local reductions in utero-placental perfusion can produce systemic changes in vascular contractility with litter-wide effects.

Our findings that *Notch2*$^{floxlflox}$;*Tpbpa-Cre* placentas failed to remodel maternal blood vessels adequately, which resulted in reduced placental perfusion, suggested that aberrations in the expression of Notch family members might be associated with PE. Another study that addressed this possibility reported expression patterns that were markedly different from those we observed at both protein and RNA levels (Cobellis et al., 2007; De Falco et al., 2007). Specifically, we found that the absence of *JAG1* expression was a common feature of perivascular and endovascular CTBs in PE. The distinctive expression pattern of *JAG1*, combined with the failure of endovascular remodeling in PE, suggested that Notch signaling is a crucial component of this unusual process. Although it is difficult to determine whether altered *JAG1* expression in PE is a prerequisite or a by-product of failed endovascular invasion, the phenotype of the *Notch2*$^{floxlflox}$;*Tpbpa-Cre* placenta supports a causal role.

In summary, we provide evidence that Notch signaling is a crucial component of the process whereby fetal trophoblast cells invade and remodel maternal blood vessels. Failure of this physiological transformation in the absence of *Notch2* is associated with reduced vessel diameter and placental perfusion, findings that support the conclusion that trophoblasts coordinate increases in maternal vascular supply through the progressive invasion and the resultant dilation of maternal vessels. The finding that peri- and endovascular CTBs often fail to express JAG1 in PE provides further evidence that defects in Notch signaling are an important part of the pathogenesis of this pregnancy complication.

**Acknowledgements**
We thank H. Stolp, M. J. Scott and G. Goldfien for assisting with human tissue collection, and acknowledge the experimental assistance of Y. Zhou, K. Red-Horse, P. A. Murphy, C. J. Shawber and D. Miniati. The *Notch2*$^{floxlflox}$ mice were a generous gift from T. Gridley. Work was supported by NIH grant HD055764. V.P. was supported by Machiah and Bikura foundation fellowships from the Israeli Science Foundation. Deposited in PMC for release after 12 months.

**Competing interests statement**
The authors declare no competing financial interests.

**Supplementary material**
Supplementary material for this article is available at
http://dev.biologists.org/lookup/suppl/doi:10.1242/dev.066589/-/DC1

**References**

**Adamson, S. L., Lu, Y., Whiteley, K. J., Holmyard, D., Hemberger, M., Pfarrer, C. and Cross, J. C.** (2002). Interactions between trophoblast cells and the maternal and fetal circulation in the mouse placenta. *Dev. Biol.* **250**, 358-373.
**Alva, J. A. and Iruela-Arispe, M. L.** (2004). Notch signaling in vascular morphogenesis. *Curr. Opin. Hematol.* **11**, 278-283.
**Amarante-Paffaro, A. M., Hoshida, M. S., Yokota, S., Goncalves, C. R., Joazeiro, P. P., Bevilacqua, E. and Yamada, A. T.** (2011). Localization of cathepsins D and B at the maternal-fetal interface and the invasiveness of the Trophoblast during the postimplantation period in the mouse. *Cells Tissues Organs* **193**, 417-425.
**Anderson, C. M., Lopez, F., Zhang, H. Y., Pavlish, K. and Benoit, J. N.** (2005). Reduced uteroplacental perfusion alters uterine arcuate artery function in the pregnant Sprague-Dawley rat. *Biol. Reprod.* **72**, 762-766.
**Basyuk, E., Cross, J. C., Corbin, J., Nakayama, H., Hunter, P., Nait-Oumesmar, B. and Lazzarini, R. A.** (1999). Murine Gcm1 gene is expressed in a subset of placental trophoblast cells. *Dev. Dyn.* **214**, 303-311.
**Bianchi, S., Dotti, M. T. and Federico, A.** (2006). Physiology and pathology of notch signalling system. *J. Cell. Physiol.* **207**, 300-308.
**Blankenship, T. N. and King, B. F.** (1996). Macaque intra-arterial trophoblast and extravillous trophoblast of the cell columns and cytotrophoblastic shell express neural cell adhesion molecule (NCAM). *Anat. Rec.* **245**, 525-531.
**Brosens, I. A., Robertson, W. B. and Dixon, H. G.** (1972). The role of the spiral arteries in the pathogenesis of preeclampsia. *Obstet. Gynecol. Annu.* **1**, 177-191.
**Cobellis, L., Mastrogiacomo, A., Federico, E., Schettino, M. T., De Falco, M., Manente, L., Coppola, G., Torella, M., Colacurci, N. and De Luca, A.** (2007). Distribution of Notch protein members in normal and preeclampsia-complicated placentas. *Cell Tissue Res.* **330**, 527-534.
**Cormier, S., Vandormael-Pournin, S., Babinet, C. and Cohen-Tannoudji, M.** (2004). Developmental expression of the Notch signaling pathway genes during mouse preimplantation development. *Gene Expr. Patterns* **4**, 713-717.
**Crews, J. K., Herrington, J. N., Granger, J. P. and Khalil, R. A.** (2000). Decreased endothelium-dependent vascular relaxation during reduction of uterine perfusion pressure in pregnant rat. *Hypertension* **35**, 367-372.
**Cross, J. C., Flannery, M. L., Blanar, M. A., Steingrimsson, E., Jenkins, N. A., Copeland, N. G., Rutter, W. J. and Werb, Z.** (1995). Hxt encodes a basic helix-loop-helix transcription factor that regulates trophoblast cell development. *Development* **121**, 2513-2523.
**Damsky, C. H., Fitzgerald, M. L. and Fisher, S. J.** (1992). Distribution patterns of extracellular matrix components and adhesion receptors are intricately modulated during first trimester cytotrophoblast differentiation along the invasive pathway, in vivo. *J. Clin. Invest.* **89**, 210-222.
**De Falco, M., Cobellis, L., Giraldi, D., Mastrogiacomo, A., Perna, A., Colacurci, N., Miele, L. and De Luca, A.** (2007). Expression and distribution of notch protein members in human placenta throughout pregnancy. *Placenta* **28**, 118-126.
**Duncan, A. W., Rattis, F. M., DiMascio, L. N., Congdon, K. L., Pazianos, G., Zhao, C., Yoon, K., Cook, J. M., Willert, K., Gaiano, N. et al.** (2005). Integration of Notch and Wnt signaling in hematopoietic stem cell maintenance. *Nat. Immunol.* **6**, 314-322.
**Fisher, S. J., Cui, T. Y., Zhang, L., Hartman, L., Grahl, K., Zhang, G. Y., Tarpey, J. and Damsky, C. H.** (1989). Adhesive and degradative properties of human placental cytotrophoblast cells in vitro. *J. Cell Biol.* **109**, 891-902.
**Goyal, R., Yellon, S. M., Longo, L. D. and Mata-Greenwood, E.** (2010). Placental gene expression in a rat 'model' of placental insufficiency. *Placenta* **31**, 568-575.
**Hamada, Y., Kadokawa, Y., Okabe, M., Ikawa, M., Coleman, J. R. and Tsujimoto, Y.** (1999). Mutation in ankyrin repeats of the mouse Notch2 gene induces early embryonic lethality. *Development* **126**, 3415-3424.
**Hamada, Y., Hiroe, T., Suzuki, Y., Oda, M., Tsujimoto, Y., Coleman, J. R. and Tanaka, S.** (2007). Notch2 is required for formation of the placental circulatory system, but not for cell-type specification in the developing mouse placenta. *Differentiation* **75**, 268-278.

**Hass, M. R., Sato, C., Kopan, R. and Zhao, G.** (2009). Presenilin: RIP and beyond. *Semin. Cell Dev. Biol.* **20**, 201-210.
**Hunkapiller, N. M. and Fisher, S. J.** (2008). Chapter 12. Placental remodeling of the uterine vasculature. *Methods Enzymol.* **445**, 281-302.
**Kopan, R. and Ilagan, M. X.** (2009). The canonical Notch signaling pathway: unfolding the activation mechanism. *Cell* **137**, 216-233.
**Lawson, N. D., Scheer, N., Pham, V. N., Kim, C. H., Chitnis, A. B., Campos-Ortega, J. A. and Weinstein, B. M.** (2001). Notch signaling is required for arterial-venous differentiation during embryonic vascular development. *Development* **128**, 3675-3683.
**Lescisin, K. R., Varmuza, S. and Rossant, J.** (1988). Isolation and characterization of a novel trophoblast-specific cDNA in the mouse. *Genes Dev.* **2**, 1639-1646.
**Levine, R. J., Hauth, J. C., Curet, L. B., Sibai, B. M., Catalano, P. M., Morris, C. D., DerSimonian, R., Esterlitz, J. R., Raymond, E. G., Bild, D. E. et al.** (1997). Trial of calcium to prevent preeclampsia. *N. Engl. J. Med.* **337**, 69-76.
**Librach, C. L., Werb, Z., Fitzgerald, M. L., Chiu, K., Corwin, N. M., Esteves, R. A., Grobelny, D., Galardy, R., Damsky, C. H. and Fisher, S. J.** (1991). 92-kD type IV collagenase mediates invasion of human cytotrophoblasts. *J. Cell Biol.* **113**, 437-449.
**Maltepe, E., Krampitz, G. W., Okazaki, K. M., Red-Horse, K., Mak, W., Simon, M. C. and Fisher, S. J.** (2005). Hypoxia-inducible factor-dependent histone deacetylase activity determines stem cell fate in the placenta. *Development* **132**, 3393-3403.
**Masumura, T., Yamamoto, K., Shimizu, N., Obi, S. and Ando, J.** (2009). Shear stress increases expression of the arterial endothelial marker ephrinB2 in murine ES cells via the VEGF-Notch signaling pathways. *Arterioscler. Thromb. Vasc. Biol.* **29**, 2125-2131.
**Matijevic, R. and Johnston, T.** (1999). In vivo assessment of failed trophoblastic invasion of the spiral arteries in pre-eclampsia. *Br. J. Obstet. Gynaecol.* **106**, 78-82.
**McCright, B., Lozier, J. and Gridley, T.** (2006). Generation of new Notch2 mutant alleles. *Genesis* **44**, 29-33.
**Miele, L.** (2006). Notch signaling. *Clin. Cancer Res.* **12**, 1074-1079.
**Morrow, D., Cullen, J. P., Cahill, P. A. and Redmond, E. M.** (2007). Cyclic strain regulates the Notch/CBF-1 signaling pathway in endothelial cells: role in angiogenic activity. *Arterioscler. Thromb. Vasc. Biol.* **27**, 1289-1296.
**Naicker, T., Khedun, S. M., Moodley, J. and Pijnenborg, R.** (2003). Quantitative analysis of trophoblast invasion in preeclampsia. *Acta Obstet. Gynecol. Scand.* **82**, 722-729.
**Nakayama, H., Liu, Y., Stifani, S. and Cross, J. C.** (1997). Developmental restriction of Mash-2 expression in trophoblast correlates with potential activation of the notch-2 pathway. *Dev. Genet.* **21**, 21-30.
**Plaks, V., Sapoznik, S., Berkovitz, E., Haffner-Krausz, R., Dekel, N., Harmelin, A. and Neeman, M.** (2010). Functional phenotyping of the maternal albumin turnover in the mouse placenta by dynamic contrast-enhanced MRI. *Mol. Imaging Biol.* **13**, 481-492.
**Red-Horse, K., Kapidzic, M., Zhou, Y., Feng, K. T., Singh, H. and Fisher, S. J.** (2005). EPHB4 regulates chemokine-evoked trophoblast responses: a mechanism for incorporating the human placenta into the maternal circulation. *Development* **132**, 4097-4106.
**Redman, C. W. and Sargent, I. L.** (2005). Latest advances in understanding preeclampsia. *Science* **308**, 1592-1594.
**Roberts, J. M. and Lain, K. Y.** (2002). Recent insights into the pathogenesis of pre-eclampsia. *Placenta* **23**, 359-372.
**Roca, C. and Adams, R. H.** (2007). Regulation of vascular morphogenesis by Notch signaling. *Genes Dev.* **21**, 2511-2524.
**Schroeter, E. H., Kisslinger, J. A. and Kopan, R.** (1998). Notch-1 signalling requires ligand-induced proteolytic release of intracellular domain. *Nature* **393**, 382-386.
**Simmons, D. G., Fortier, A. L. and Cross, J. C.** (2007). Diverse subtypes and developmental origins of trophoblast giant cells in the mouse placenta. *Dev. Biol.* **304**, 567-578.
**Simmons, D. G., Rawn, S., Davies, A., Hughes, M. and Cross, J. C.** (2008). Spatial and temporal expression of the 23 murine Prolactin/Placental Lactogen-related genes is not associated with their position in the locus. *BMC Genomics* **9**, 352.
**Swift, M. R. and Weinstein, B. M.** (2009). Arterial-venous specification during development. *Circ. Res.* **104**, 576-588.
**Villa, N., Walker, L., Lindsell, C. E., Gasson, J., Iruela-Arispe, M. L. and Weinmaster, G.** (2001). Vascular expression of Notch pathway receptors and ligands is restricted to arterial vessels. *Mech. Dev.* **108**, 161-164.
**Wang, H. U., Chen, Z. F. and Anderson, D. J.** (1998). Molecular distinction and angiogenic interaction between embryonic arteries and veins revealed by ephrin-B2 and its receptor Eph-B4. *Cell* **93**, 741-753.
**Wang, X. L., Fu, A., Raghavakaimal, S. and Lee, H. C.** (2007). Proteomic analysis of vascular endothelial cells in response to laminar shear stress. *Proteomics* **7**, 588-596.
**Weihofen, A., Lemberg, M. K., Friedmann, E., Rueeger, H., Schmitz, A., Paganetti, P., Rovelli, G. and Martoglio, B.** (2003). Targeting presenilin-type aspartic protease signal peptide peptidase with gamma-secretase inhibitors. *J. Biol. Chem.* **278**, 16528-16533.
**Weinmaster, G.** (1998). Notch signaling: direct or what? *Curr. Opin. Genet. Dev.* **8**, 436-442.
**Williams, C. K., Li, J. L., Murga, M., Harris, A. L. and Tosato, G.** (2006). Up-regulation of the Notch ligand Delta-like 4 inhibits VEGF-induced endothelial cell function. *Blood* **107**, 931-939.
**Winn, V. D., Gormley, M., Paquet, A. C., Kjaer-Sorensen, K., Kramer, A., Rumer, K. K., Haimov-Kochman, R., Yeh, R. F., Overgaard, M. T., Varki, A. et al.** (2009). Severe preeclampsia-related changes in gene expression at the maternal-fetal interface include sialic acid-binding immunoglobulin-like lectin-6 and pappalysin-2. *Endocrinology* **150**, 452-462.
**Witt, C. M., Won, W. J., Hurez, V. and Klug, C. A.** (2003). Notch2 haploinsufficiency results in diminished B1 B cells and a severe reduction in marginal zone B cells. *J. Immunol.* **171**, 2783-2788.
**Zhong, T. P., Childs, S., Leu, J. P. and Fishman, M. C.** (2001). Gridlock signalling pathway fashions the first embryonic artery. *Nature* **414**, 216-220.
**Zhou, Y., Fisher, S. J., Janatpour, M., Genbacev, O., Dejana, E., Wheelock, M. and Damsky, C. H.** (1997). Human cytotrophoblasts adopt a vascular phenotype as they differentiate. A strategy for successful endovascular invasion? *J. Clin. Invest.* **99**, 2139-2151.
**Zhou, Y., McMaster, M., Woo, K., Janatpour, M., Perry, J., Karpanen, T., Alitalo, K., Damsky, C. and Fisher, S. J.** (2002). Vascular endothelial growth factor ligands and receptors that regulate human cytotrophoblast survival are dysregulated in severe preeclampsia and hemolysis, elevated liver enzymes, and low platelets syndrome. *Am. J. Pathol.* **160**, 1405-1423.
**Zhou, Y., Bellingard, V., Feng, K. T., McMaster, M. and Fisher, S. J.** (2003). Human cytotrophoblasts promote endothelial survival and vascular remodeling through secretion of Ang2, PlGF, and VEGF-C. *Dev. Biol.* **263**, 114-125.
**Zhou, Y., Bianco, K., Huang, L., Nien, J. K., McMaster, M., Romero, R. and Fisher, S. J.** (2007). Comparative analysis of maternal-fetal interface in preeclampsia and preterm labor. *Cell Tissue Res.* **329**, 559-569.